LOCAL SITE EFFECTS AT THE NEVADA SEISMIC ARRAY (NVAR)

Eugene T. Herrin, Petru T. Negraru, Paul Golden, Carl Mulcahy

Southern Methodist University

Sponsored by Defense Threat Reduction Agency

Contract No. DTRA01-00-C-0093

ABSTRACT

In most cases array processing techniques are based on homogeneous structure assumptions, which is not always true. The output of a frequency-wave number analysis, based on the Fourier Transform, which is often used in processing raw data, will be strongly biased if all the stations do not have the same frequency content. In spite of the evidence that individual station corrections must be applied, corrections are not widely used. Often a simple relief correction is believed to account for all the local site effects.

The goal of this study is to present and, if possible, to explain the anomalous amplitude variations that are recorded at the Nevada Seismic Array (NVAR). Narrow-band frequency-dependent amplitudes were measured for both regional and teleseismic phases. Differences in source function (corner frequency) and attenuation account for the frequency content of different phases. Typically regional events allow observation from 0.5 to 16 Hz (0.5-1 Hz, 2-4 Hz, 4-8 Hz and 8-16 Hz) and teleseismic from 0.12 to 4 Hz (0.12-0.25 Hz, 0.25-0.5 Hz, 0.5-1 Hz, 1-2 Hz and 2-4 Hz). Although there are differences, particularly at high frequency, similar patterns are recognized for all phases. The most striking feature is the much larger amplitude exhibited by NV04 at frequencies 1-2 Hz and 2-4 Hz. Across the whole array, the variation in this frequency band can be higher than a factor of 8. The amplitude variation between NV04 and NV01, stations located only 500 meters apart can reach a factor of six. At higher frequency, 4-8 Hz and 8-16 Hz, NV09 dominates, its amplitude being occasionally more than one order of magnitude larger than the rest of the stations. No azimuth and distance dependence was found for these effects, which implies the absence of any organized dipping structure.

Taking advantage of the co-located seismic and experimental infrasound arrays, the seismic responses for propagating pressure waves were analyzed. The effects are larger, possibly because of the higher frequency (shorter wavelength) of the infrasound signals. The presence of the same amplitude effects leads to the conclusion that the structure responsible for these effects is shallow, being up to a few tens of meters.

To better understand the shallow structure, refraction profiles will be carried out in the field. Considering the depth of seismometer emplacement, true velocities can be obtained for the upper 12 meters using the short-period seismometer as a stationary receiver and moving the source further away from it, in a “walk-away” technique. In this way the presence of a low-velocity layer in the first 12 meters that may exist near site NV04 can be determined. It is desired to investigate the structure to a depth of 30 meters, the standard depth used by engineers to classify site characteristics.

OBJECTIVE

The objective of this study is to present and explain the effects that occur at the Nevada Seismic Array (NVAR) due to variations in the local geology. Common array processing techniques are based on homogeneous geological structure assumptions, which is clearly a simplification of the problem. In processing raw data the time-space domain is transformed in frequency-wave number domain by computing two-dimensional Fourier Transforms. The azimuth and phase velocity for the desired time window at the desired frequency are found by looking for the peak in power. Such an approach yields satisfactory results when the input time functions do not exhibit large spectral variations. This is usually the case in areas with uniform geological structure. Therefore, if an array exhibits large spectral variations, the outcome of f-k processing will be biased, and even the detection capability of the array could be lowered. At areas with large topographic variations, sometimes a simple relief correction is applied before processing, to account for the local site effects, but such an approach takes into account the topography rather than the geology.

RESEARCH ACCOMPLISHED

Berteussen (1974) was the first to observe and discuss amplitude variations at a seismic array. Explaining the travel-time anomalies recorded beneath several seismic arrays (NORSAR, LASA) in terms of scattering waves due to lower crust – upper mantle heterogeneities was the focus at the time. Additional papers were published discussing this subject (Aki, 1973; Capon 1974, Berteussen *et al* 1975; Berteussen 1975). More recently, the array calibration work has shifted toward experimental calibration (Tibuleac *et al*, 2001). A set of station corrections is developed empirically, to improve the location capabilities of the array. This approach yields better results, but it won't improve the detection capability for the whole array. Experience gained from the NORSAR array led to the installation of the small aperture NORESS array, which has a detection capability higher than NORSAR, for sources located close to the Semipalatinsk Test Site, although it was built at the location of one of the NORSAR subarrays.

The Nevada Seismic Array (NVAR) was installed in December 1998 by Southern Methodist University. The location of the array was chosen following negotiations between a team of experts from the USA and Russia. It was decided that one of the three-component stations would be located in the Black Butte mine, on the former setting of the station MNV (Mina, Nevada) for which historically recorded nuclear explosions exist (Figure 1). Although the array fulfills its mission very well, to provide coverage for the Nevada Test Site (NTS), the final location in a very

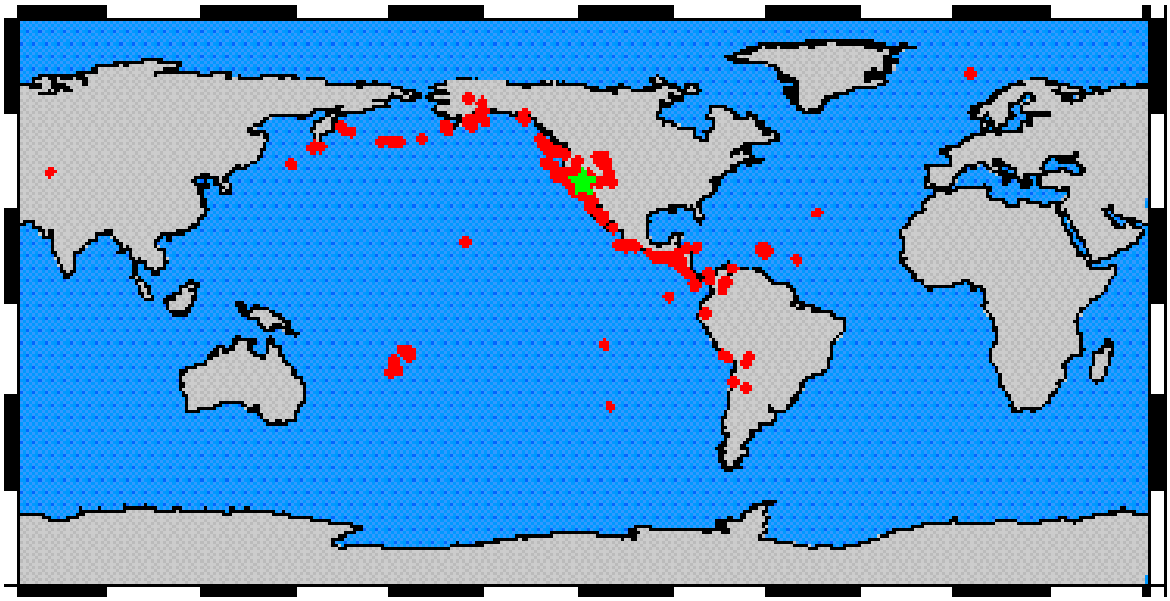

Figure 1. Position of earthquakes used in this study. The green star represents the location of the Nevada Seismic Array (NVAR)

complex geology led to unusual site effects, which raised the problem of determining an optimum array processing technique. The array consists of three broadband, three-component stations and ten short-period vertical stations. A weather station monitoring temperature, wind speed, wind direction, atmospheric pressure and relative humidity is located within the array. The present study is restricted only to the short-period stations, with the main focus on the inner ring of the array whose stations are co-located with an experimental infrasound array. More than half of the stations (stations NV01, NV02, NV03, NV05, NV06 and NV10) are located in the steeply dipping limestone of the Luning formation (Figure 2). These rocks were deposited during the late Triassic Period and can reach a thickness greater than 2 km close to the array. Site NV04 is located in lithified terrace gravels of Tertiary age. Site NV07 is located in the Dunlop formation, which comprises a very fine-grained sandstone, but the formation is variable within the region and can include shale and volcanic assemblages. Site NV09 is located in a Tertiary basalt flow, whereas site NV08 is sited in a Cretaceous granitic intrusive body.

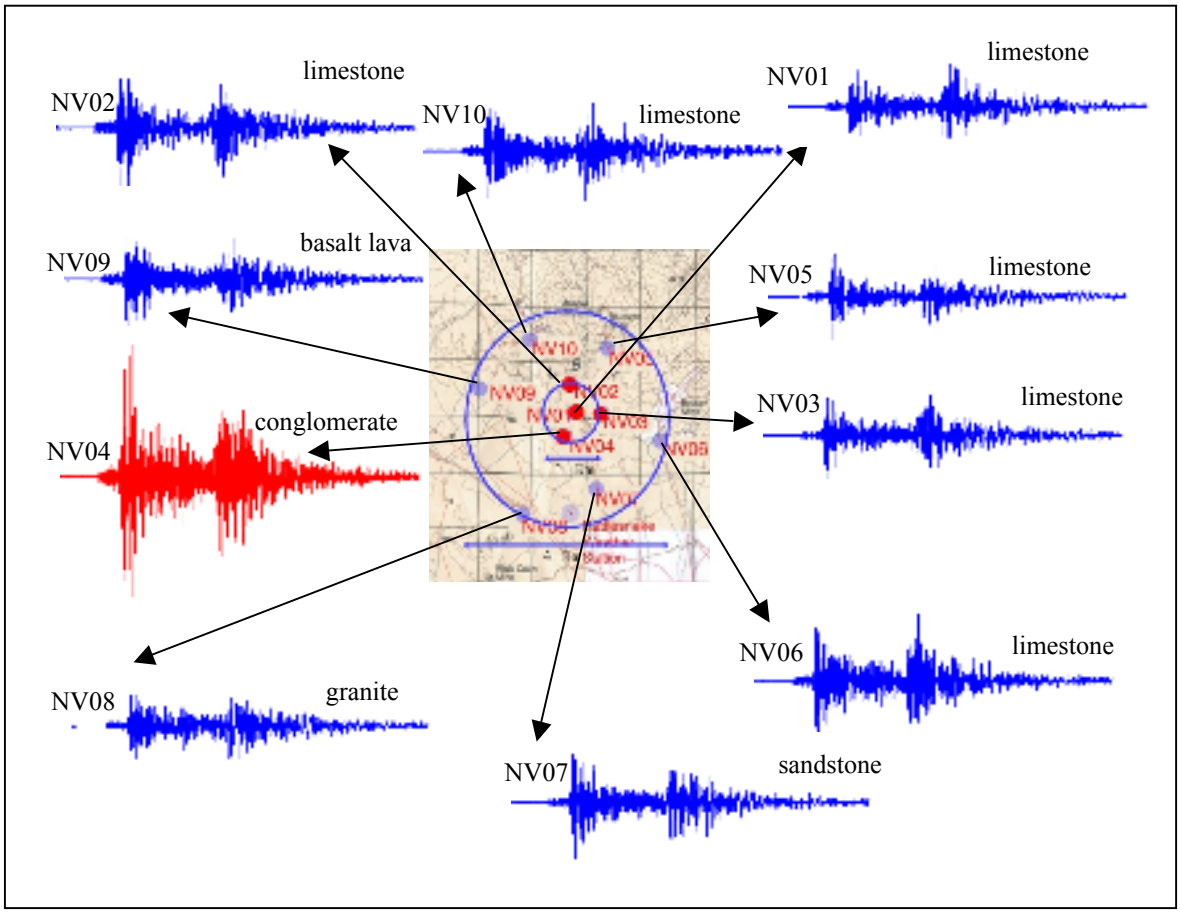

Figure 2. Detailed map of the NVAR array. The waveforms represent raw data recorded at NVAR at each of the short-period stations. The magnitude 5.7 earthquake occurred in California at a distance of 478 km. All the traces shown here are at the same scale. The red trace is channel NV04, located in Tertiary conglomerate, which exhibits the largest amplitude by a factor of three in this particular case.

To illustrate the local site effects encountered at NVAR, narrow-band frequency-peak accelerations were measured for both regional and teleseismic phases (Pn, Pg, Lg and teleseismic P). Although we desired observations in the same frequency band, variations in source functions and attenuation did not always allow this. In order to have a good signal-to-noise (SNR) ratio, most of the teleseismic earthquakes must have a magnitude higher than 5. Because the larger the earthquake, the lower the corner frequency, there is not too much energy above 4 Hz and secondly the high-frequency attenuation is much greater than at lower frequencies. Typically, teleseismic earthquakes, located at distances ranging from 24 to 90 degrees, allow observations from 0.12 to 4 Hz (0.12-0.25, 0.25-0.5, 0.5-1, 1-2 Hz) and regional events from 0.5 to 16 Hz (0.5-1, 1-2, 2-4, 4-8, 8-16 Hz).

In order to have a good azimuthal coverage, some earthquakes with lower magnitudes were included. The data consist of 75 teleseismic events and 213 regional earthquakes with magnitude between 3.5 and 7 (Figure 1). A fourth-order recursive Butterworth filter was applied for each frequency band, and the peak acceleration was measured from the envelope functions computed using Hilbert Transforms. In general the final results are relative to a particular channel, and thus most of the results will be equivalent for displacement, velocity and acceleration.

Taking advantage of the co-located seismic and experimental infrasound arrays, the seismic responses to propagating pressure waves were analyzed. The seismo-acoustic signals were detected by estimating the correlation coefficients at zero lag between seismic and acoustic envelope functions for a sliding 10-s window. Because the shorter the window, the higher the correlation coefficients for seismic and infrasound noise, a trade-off between window length and correlation threshold was achieved. The time length of most signals, which in general do not exceed a few seconds, was also taken into account. Empirically, the 10-s window and a detection threshold of 0.5 gave good results. Typically the noise for such a window length will have correlation coefficients below 0.3. Signals with good SNR have correlation coefficients above 0.5. The maximum correlation coefficient was 0.99, for a signal recorded on channel NV04. A detection was declared if there were correlation coefficients above 0.5 for at least three stations. Although this method works well for NVAR, it is not expected to work in the same way for all stations in the western US, but a similar approach can be used to make a detector at each particular array (or site). From 07/18/2001 to 08/30/2001 there were over 100 signals detected in this manner. Afterwards the amplitude was measured in the same way as the seismic signals, except that instead of peak acceleration, we calculated the root mean square value for the first three seconds of the signal. The bandpass filters used were similar to the filters used for regional events.

Background noise studies were also conducted. Ten-minute-long noise samples were chosen for different wind velocities. The sample was chosen so that the wind velocity had small variation during the time of interest. From every four-hour block, one time frame was chosen. The Welch Block Averaging method (Welch, 1967) was then applied to yield power spectral density estimates. The length of each data block was 512 points to constrain the individual estimates to frequencies greater than 0.1 Hertz. The individual blocks in each sample record were overlapped by 50 % and a Hanning window was used to reduce the variance of the power spectral density estimate.

CONCLUSIONS AND RECOMMENDATIONS

Figure 3 represents the spatial variations in ground motion peak acceleration for teleseismic P, Pn, Pg and Lg phases. Although there are differences, most notably at high frequencies, the patterns are very similar. The common feature for all analyzed phases is the much larger amplitude recorded at channel NV04 for frequency bands 1-2 Hz and 2-4 Hz. For stations NV01 and NV04, located only 500 m apart, the difference in peak acceleration can be as large as a factor of six. The largest difference across the whole array occurs usually for stations NV04 (largest amplitude) and NV05 (smallest amplitude), and could be higher than a factor of eight. At longer periods (0.12 – 0.25 Hz and 0.25 – 0.5 Hz), the signal is very similar, the variations being less than a factor of two. At higher frequencies (4 – 8 Hz and 8 –16 Hz), NV09 exhibits the largest amplitude, its peak acceleration being sometimes more than one order of magnitude larger than NV07.

No significant azimuthal or distance pattern has been found for this effect (Figure 4), which suggests the lack of any organized dipping structure. This conclusion is also supported by a previous calibration study (Tibuleac *et al*, 2001). This would suggest that the anomalous structure is flat to the first order.

The effects are larger for the pressure waves (Figure 5), possibly because of the higher frequency (shorter wavelength) of the infrasound signals. For approximately the same pressure levels, the variations in amplitude can be larger than a factor of 20. In general the amplitude recorded on the seismic channels for NV01 and NV03 are similar, which suggests the presence of the same physical properties beneath these two stations. NV04 always exhibits the largest amplitude and NV02, although located in the same geology as NV01 and NV03 can exhibit amplitudes larger than a factor of 10 when compared with NV02 and NV03.

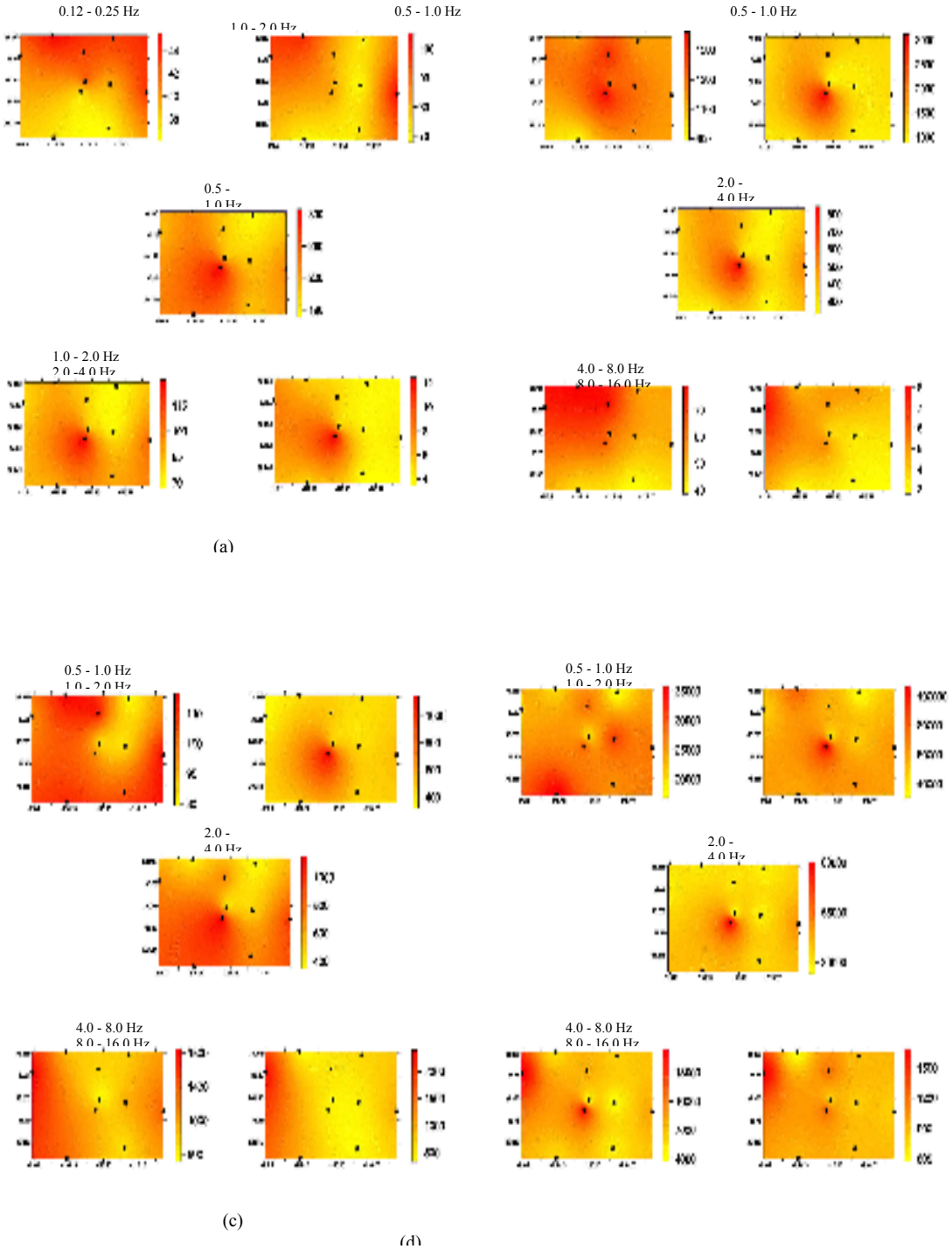

Figure 3. Spatial variations in ground motion peak acceleration of teleseismic P (a), Pn (b), Pg(c) and Lg (d). The black dots represent the position of each individual station. The units of the map are nm/s^2.

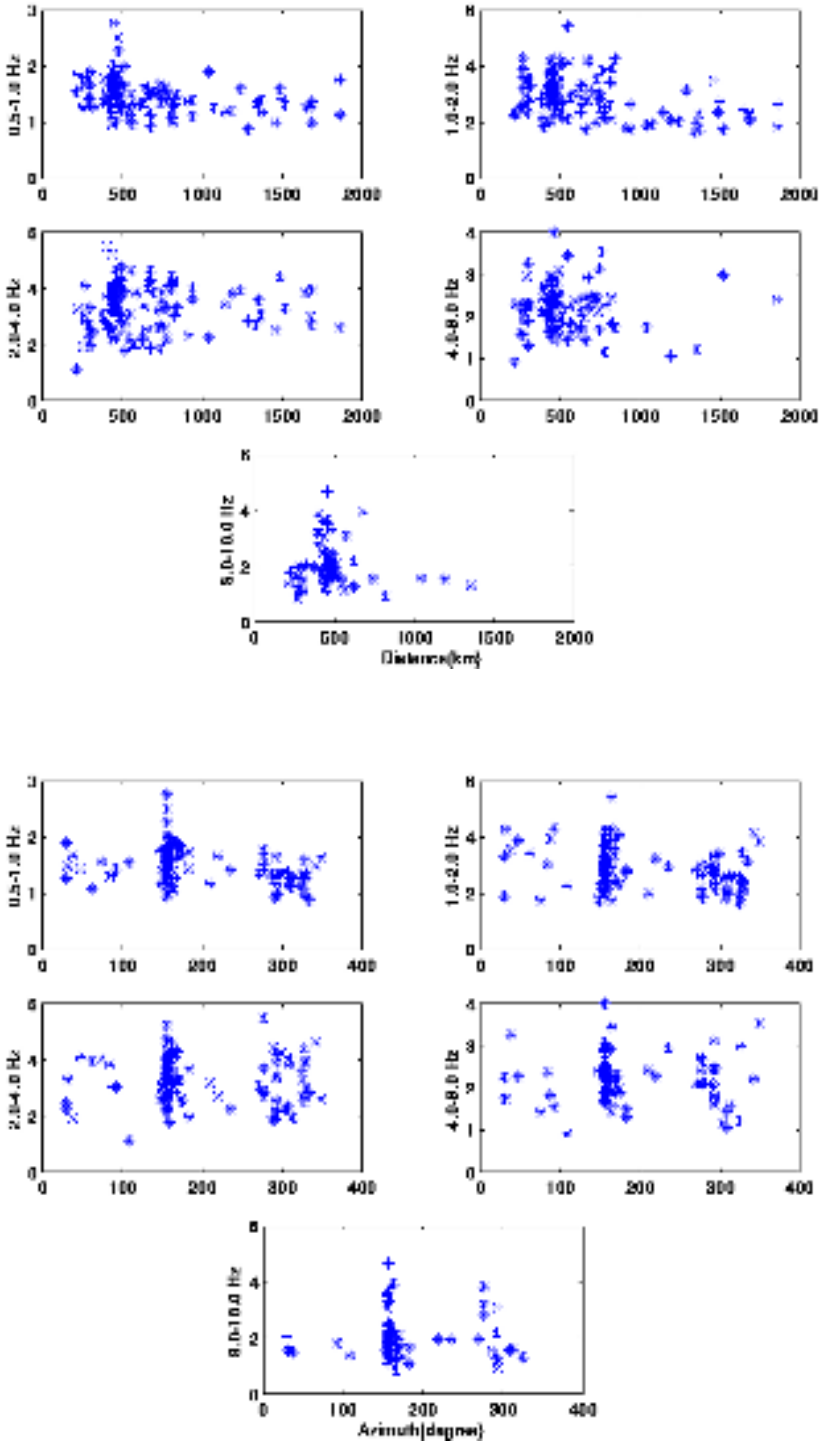

Figure 4. NV04/NV01 peak acceleration ratio for regional events. No pattern has been found as a function of distance (upper plot) or azimuth (lower plot). These two stations situated only 500 m apart exhibit variations as big as a factor of six in peak acceleration. The largest variation across the whole array for this set of events occurred for NV04 (largest acceleration) and NV05 (lowest acceleration) and was more than a factor of eight.

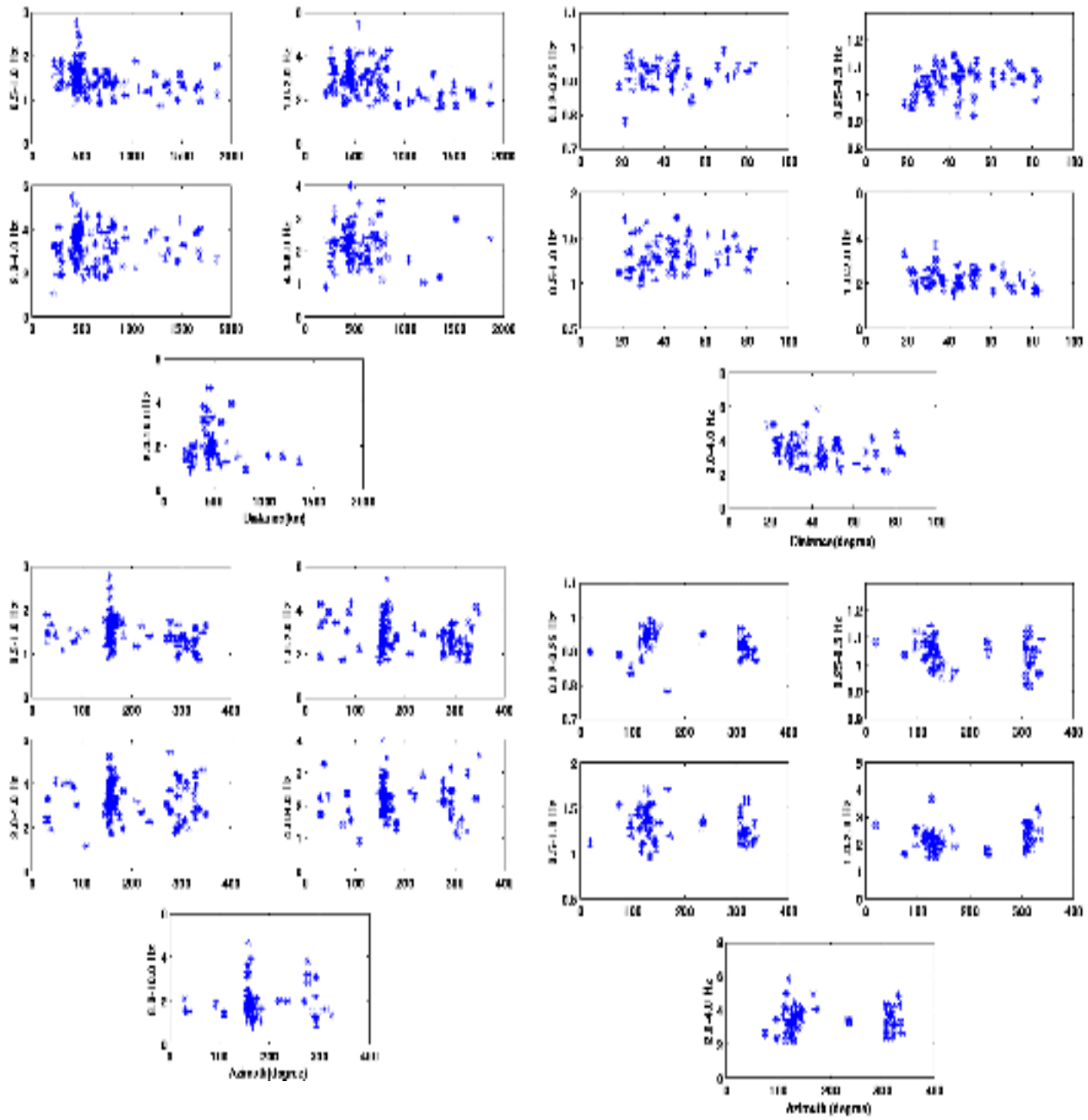

Figure 5. NV04/NV01 peak acceleration ratio for teleseismic events. The results are similar to the regional events. The maximum peak acceleration variations (for stations NV01 and NV04) is close to a factor of six, and the maximum variation across the whole array is close to a factor of eight

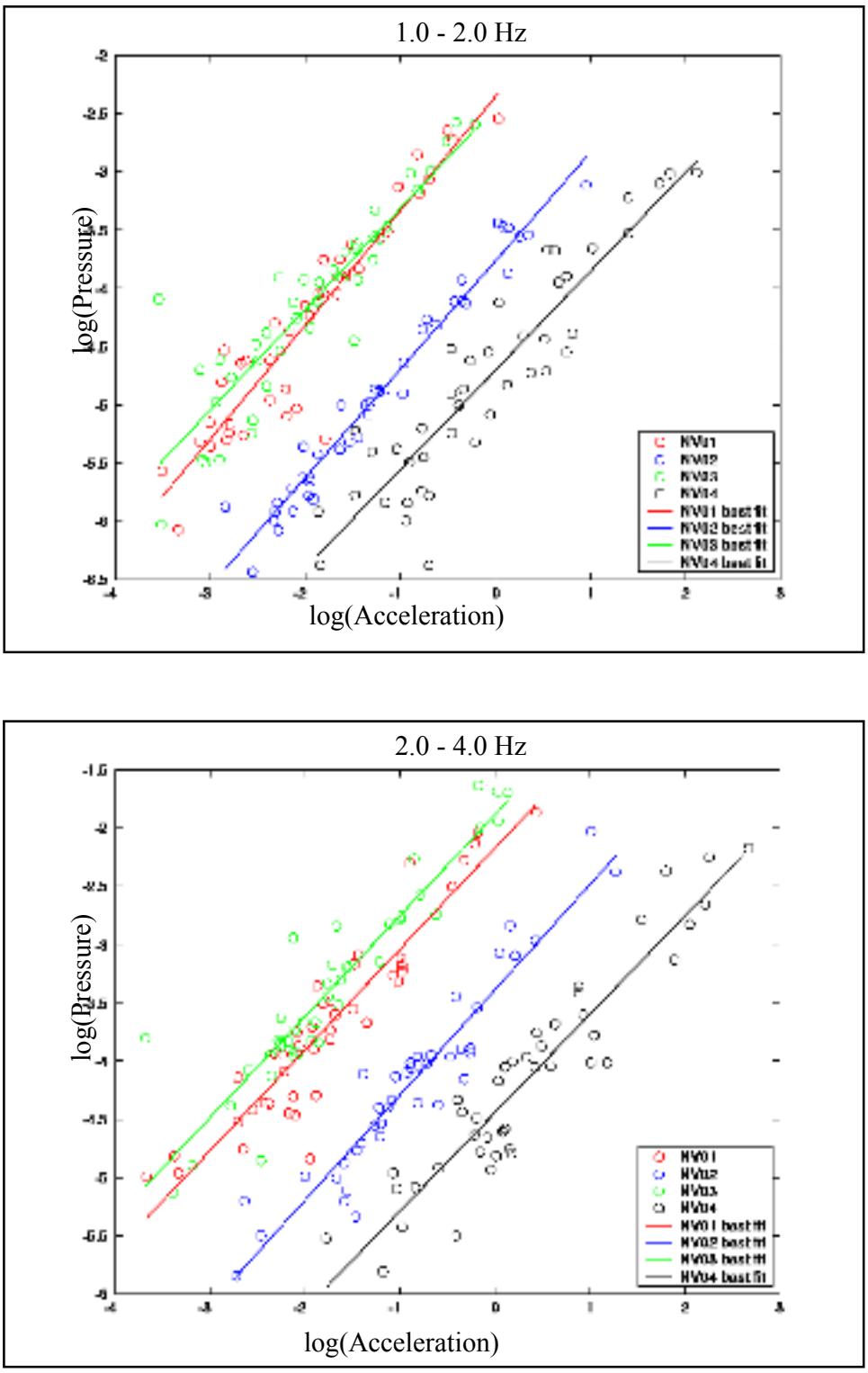

Figure 6. RMS Pressure versus RMS Acceleration for seismo-acoustic events. The data below 1 Hertz is contaminated by noise, and above 4 Hertz the response of the infrasound sensor hoses can further bias the measurements. The difference between NV01, NV03 and NV02 is likely to be due to the weathering effects. The difference between NV04 and the rest of the channels is due to the change in local geology. The Pressure Units are Pa; the acceleration units are nm/s^2.

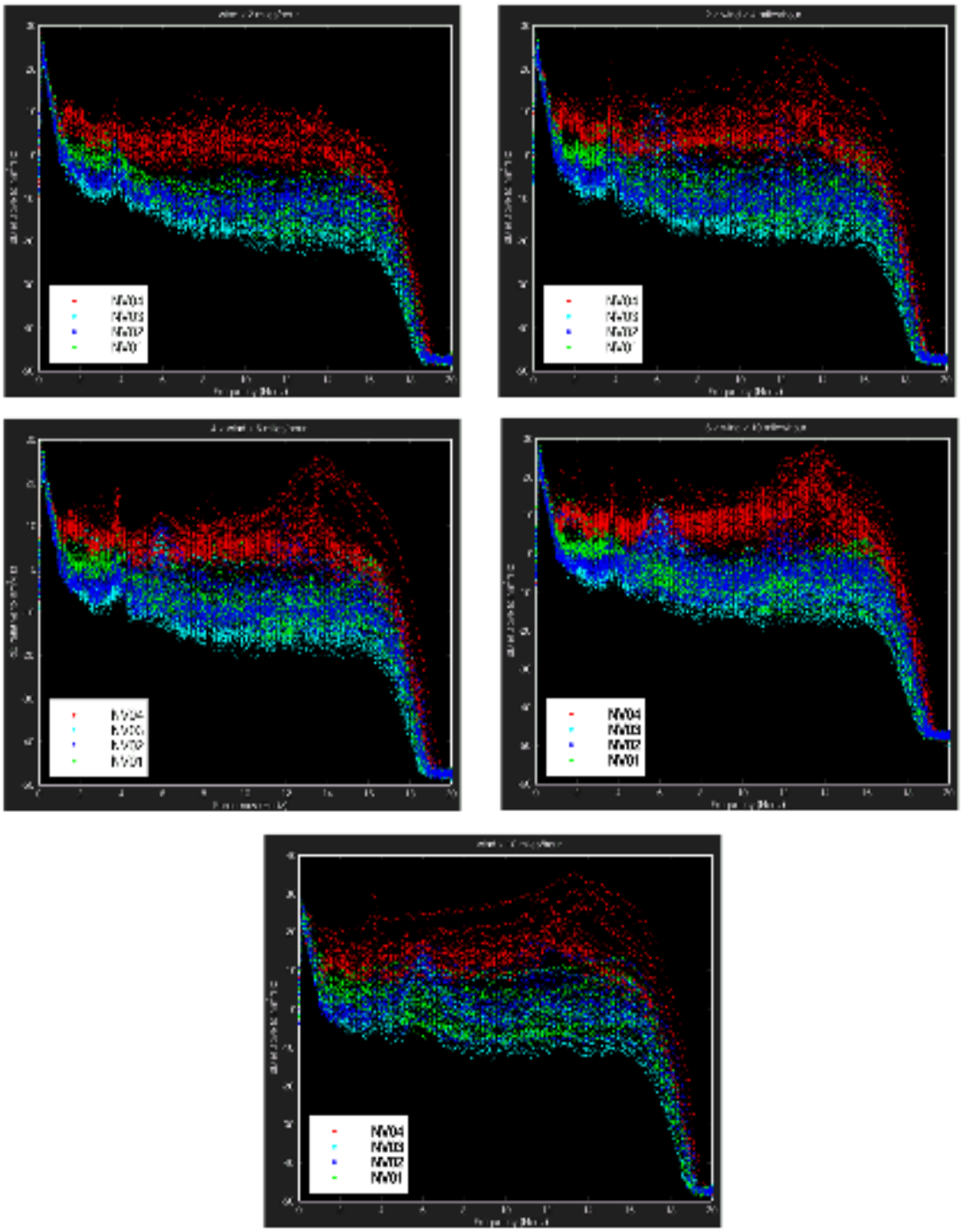

Figure 7. Power Spectrum Density Function for a suite of 160 noise samples. Here are shown only the elements of the inner array (NV01, NV02, NV03 and NV04). The wind velocities are: less than 2 miles/hour (upper plot left), 2-4 miles/hour (upper plot right), 4-6 miles/hour (middle plot left), 6-10 miles/hour (middle plot right), above 10 miles /hour (lower plot).

These effects are not related to or influenced by atmospheric noise. The noise analyses (Figure 7) show that the atmospheric noise is more important at frequencies above 1 Hz. The median noise difference for NV04 and NV01 between the peak at around 6 Hz exhibited by NV01 and the peak at around 14 Hz exhibited by NV04 is approximately constant and is around 10 dB, regardless of wind strength. The maximum difference can reach 25 dB. At 1 Hz the median difference is 5 dB. The broad peaks that appear around 14 Hz (for NV04) and around 6 Hz (for NV03 and NV01) represent the combined effect of geology and topography.

To fully understand the geological structure responsible for these site effects refraction profiles will be carried out in the field. Taking advantage of the depth of the seismometers, true velocities can be obtained for the upper 40 feet using the seismometer as a static receiver and moving the source away from it in a "walk-away" technique. In this way the presence of a low-velocity layer that may exist near site NV04 can be detected. Additionally, shear velocity refraction profiles might be necessary because of the complicated geology. It is desired to investigate the structure to a depth of at least 30 m, the standard depth used by engineers to classify site characteristics.

REFERENCES

Aki K (1973) Scattering of P-waves under the Montana LASA, *J.Geophys. Res*. **78**, 1334-1346

Berteussen (1975) Crustal structure and P-wave travel time anomalies at NORSAR, *J. Geophys*., **41**, 71-84

Berteussen (1975) P-wave amplitude variability at NORSAR*, J. Geophys*. **41**, 595-613

Berteussen K. A., Christoffersson A., Husebye E. S. and Dahles A. (1975), Wave scattering theory in analysis of P-wave anomalies at NORSAR and LASA, *Geophys. J. R astr. Soc*. **42**, 403-417

Capon J. (1973), Characterization of crust and upper mantle structure under LASA as a random medium, *Bull. Seism. Soc. Am*. **64**, 235-266

NVAR Certification Manual (1999) prepared for the Preparatory Commission for the Comprehensive Nuclear-Test-Ban Treaty Organization Provisional Technical Secretariat International Monitoring System Division.

Tibuleac I. M., Herrin E. T. and Negraru P. T. (2001), Calibration studies at NVAR*, Seism. Res. Let*., **72**, 754